Cell PRESS
Open ACCESS

EXTENDED EXPERIMENTAL PROCEDURES

Cloning and Protein Purification

All proteins were amplified from *S. cerevisiae* genomic DNA and cloned into pET-based vectors with N-terminal, TEV-protease cleavable His_6 tags. For in vitro expression in rabbit reticulocyte lysate (discussed later), a Kozak sequence (CCGCCACC) was added 5′ to the start codon and plasmid DNA was used directly. For coexpression, polycistronic expression cassettes were assembled by PCR, with one subunit tagged with a TEV protease-cleavable His_6 tag. Proteins were expressed in *E. coli* strain Rosetta 2 pLysS (EMD Biosciences) or, for constructs including Hrr25, SOLUBL21 (Genlantis); expression was induced with IPTG for 16–20 hr at 20°C. Proteins were purified by Ni^{2+} affinity (Ni-NTA; QIAGEN) and ion-exchange (Hitrap Q HP or SP HP; GE Healthcare) chromatography, and then His_6 tags were cleaved by incubation with TEV protease (Kapust et al., 2001) at 4°C overnight, and the protein was further purified by gel filtration (Superdex 200; GE Healthcare). Proteins were concentrated and stored at 4°C for crystallization or frozen at −80°C for pulldowns.

For mass spectrometry analysis, wild-type $Hrr25^{1–394}$ was expressed and purified as described earlier, either in isolation or coexpressed with $Mam1^{87–191}$. Samples were separated by SDS-PAGE and Coomassie blue-stained, and bands were excised. Bands were then crushed, trypsinized, and examined by liquid chromatography-tandem mass spectrometry (LC/MS/MS; Taplin Mass Spectrometry Facility, Harvard Medical School).

For sedimentation equilibrium analytical ultracentrifugation (AUC), proteins were spun in a Beckman Optima XL-A centrifuge at three speeds, which varied with the expected molecular weight of the protein/complex. For each protein, nine curves (three speeds × three protein concentrations) were fit together to a single-species model using Origin (Beckman Coulter Inc.). For size-exclusion chromatography-linked multi-angle light scattering (SEC-MALS), proteins were separated on a size exclusion column (Wyatt Technology WTC-03S5 or GE Life Sciences Superdex 200 10/300 GL), their light scattering and refractive index profiles collected by miniDAWN TREOS and Optilab T-rEX detectors (Wyatt Technology), respectively, and their molecular weights were calculated using ASTRA v. 6 software (Wyatt Technology).

Pulldown Assays

In vitro expression of bait proteins and pulldown assays were performed essentially as described (Corbett et al., 2010). Briefly, plasmid DNA was added to a coupled transcription/translation kit (TNT T7; Promega) to express either untagged or MBP-fused prey proteins labeled with $^{[35]}$S-methionine. Ten μl of transcribed protein mix was incubated with 10 μg bait protein in 50 μl buffer (20 mM HEPES, pH 7.5, 150 mM NaCl, 20 mM imidazole, 5% glycerol, 1 mM dithiothreitol (DTT), 0.1% NP-40) for 90 min at 4°C, then 15 μl Ni-NTA beads were added, and the mixture was incubated a further 45 min. Beads were washed three times with 0.5 ml buffer, then eluted with 25 μl elution buffer (2× SDS-PAGE loading dye plus 400 mM imidazole) and boiled. Samples were run on SDS-PAGE, dried, and scanned with a phosphorimager.

Crystallization and Structure Determination

For crystallization, purified Csm1:$Mam1^{221–290}$ at 8–10 mg/ml was dialyzed into 20 mM HEPES, pH 7.5, 150 mM NaCl, and 1 mM DTT. Protein was mixed 1:1 in hanging drop format with well solution containing 100 mM HEPES, pH 7.5, 100–150 mM $MgCl_2$, and 6%–9% PEG 4000. Crystals (hexagonal bipyramids ~100 × 100 × 300 μm) were cryoprotected by addition of 25% PEG 400 and flash-frozen in liquid nitrogen.

All data sets were collected on NE-CAT beamlines 24ID-C and 24ID-E at the Advanced Photon Source at Argonne National Laboratory. The structure of Csm1:$Mam1^{221–290}$ was determined by molecular replacement with PHASER (McCoy et al., 2007), using the structure of full-length Csm1 (PDB ID 3N4X) as a search model. The crystals have same space group ($P3_121$) and the same packing as our previous crystals of full-length Csm1 alone, but they contain only one Csm1 dimer per asymmetric unit instead of two; Mam1 binding prevents the packing of the second Csm1 dimer. We manually built Mam1 residues 223–263 into density-modified difference maps and refined, B-factor sharpened $2F_o$-F_c maps, using the program Coot (Emsley et al., 2010), and refined the structure using phenix.refine (Adams et al., 2010) (see Table S3 for statistics).

SUPPLEMENTAL REFERENCES

Adams, P.D., Afonine, P.V., Bunkóczi, G., Chen, V.B., Davis, I.W., Echols, N., Headd, J.J., Hung, L.-W., Kapral, G.J., Grosse-Kunstleve, R.W., et al. (2010). PHENIX: a comprehensive Python-based system for macromolecular structure solution. Acta Crystallogr. D Biol. Crystallogr. *66*, 213–221.

Emsley, P., Lohkamp, B., Scott, W.G., and Cowtan, K. (2010). Features and development of Coot. Acta Crystallogr. D Biol. Crystallogr. *66*, 486–501.

Kapust, R.B., Tözsér, J., Fox, J.D., Anderson, D.E., Cherry, S., Copeland, T.D., and Waugh, D.S. (2001). Tobacco etch virus protease: mechanism of autolysis and rational design of stable mutants with wild-type catalytic proficiency. Protein Eng. *14*, 993–1000.

McCoy, A.J., Grosse-Kunstleve, R.W., Adams, P.D., Winn, M.D., Storoni, L.C., and Read, R.J. (2007). Phaser crystallographic software. J. Appl. Cryst. *40*, 658–674.

Waterhouse, A.M., Procter, J.B., Martin, D.M.A., Clamp, M., and Barton, G.J. (2009). Jalview Version 2—a multiple sequence alignment editor and analysis workbench. Bioinformatics *25*, 1189–1191.

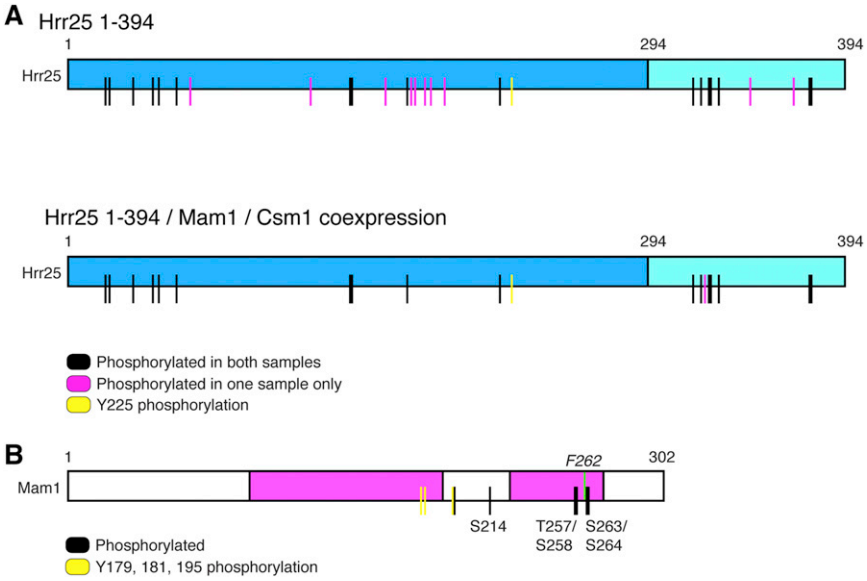

Figure S1. Mass Spectrometry Characterization of Monopolin Phosphorylation, Related to Figure 1

(A) Summary of Hrr25 autophosphorylation sites identified by mass spectrometry. Top: Hrr25$^{1-394}$ expressed alone in *E. coli*. Bottom: Combination of results from two co-expression samples: Hrr25$^{1-394}$:Mam1$^{87-302}$:Csm1, and Hrr25$^{1-394}$:Mam1$^{1-302}$:Csm1. Black bars indicate phosphorylation sites shared by Hrr25 alone and Hrr25 co-expressed with other components; magenta bars show sites found only in one sample; the yellow bar shows Tyr225, phosphorylated in both samples.

(B) Summary of Hrr25 phosphorylation sites on Mam1 identified by mass spectrometry. Yellow lines indicate weak phosphorylation on Tyr179, 181, and 195. Ser214 was the most strongly phosphorylated site we detected in either Mam1 or Hrr25; phosphorylated peptides containing Ser214 were consistently detected at equivalent/higher levels than non-phosphorylated peptides (Table S1). Phe262, which anchors the interaction of Mam1 with Csm1's kinetochore protein-binding patch, is shown in green for reference; see Figure 3.

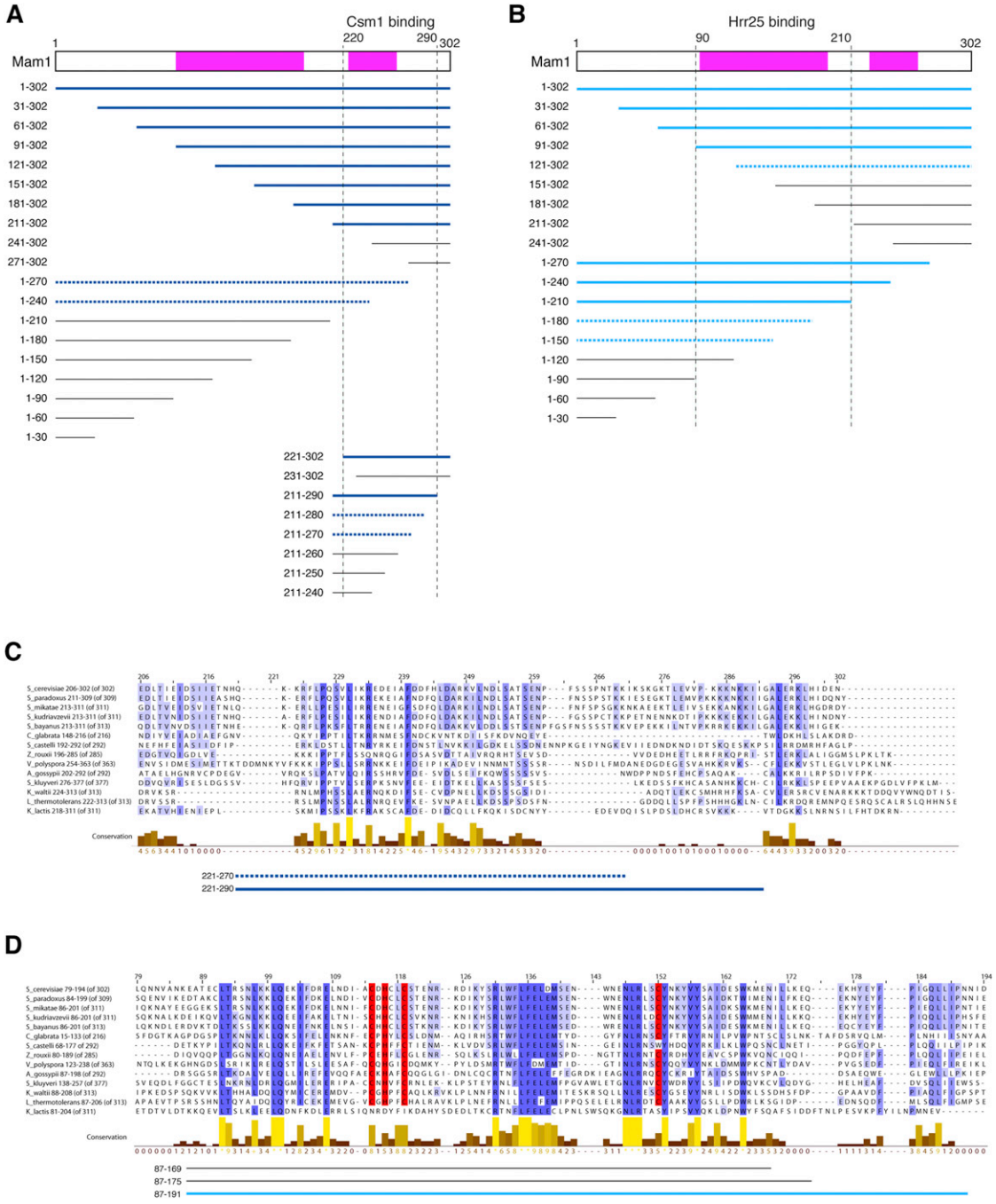

Figure S2. In Vitro Characterization of Monopolin Subcomplexes, Related to Figure 1

(A) Summary of pulldown experiments measuring Mam1 fragment binding by Csm1. Solid blue lines indicate strong interaction of a fragment with Csm1, dashed blue indicates weak interaction, and thin black indicates no interaction. The minimal binding region, residues 221-290, is highlighted.

(B) Summary of pulldown experiments measuring Mam1 fragment binding by Hrr25. The minimal binding region identified by pulldowns, residues 90-210, is highlighted.

(C) Multiple sequence alignment of the Mam1 C-terminal region, showing two constructs of Mam1 (221-270 and 221-290) tested by co-expression with Csm1.

(D) Multiple sequence alignment of the Mam1 middle region, showing a conserved CxHxxCx$_{32-38}$C motif (residues 114, 116, 119, and 152 in *S. cerevisiae*) in red that suggests possible zinc-ion binding; the codon for *S. castelli* residue 135, annotated as TGG (Trp), differs by one base from the Cys codons TGT or TGC, and may thus represent either a recent mutation in this species or a sequencing error. *K. lactis* lacks the CxHxxCx$_{32-38}$C motif entirely. Shown below are three constructs of Mam1 (87-169, 87-175, and 87-191) tested by co-expression with Hrr25. Alignments created with Jalview (Waterhouse et al., 2009).

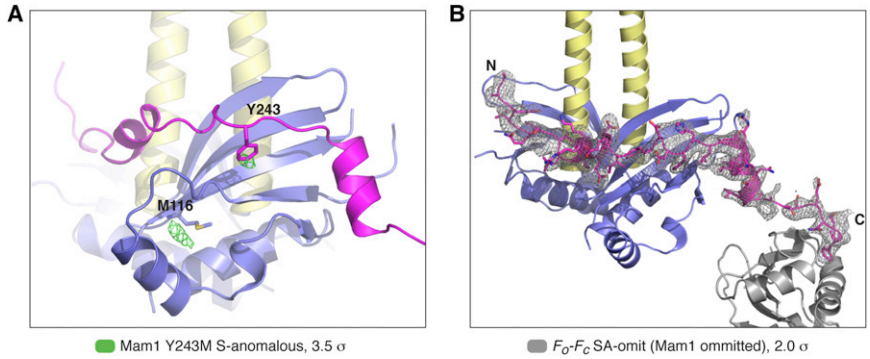

Figure S3. Electron Density Maps, Related to Figure 2

(A) Anomalous difference electron density map, contoured at 3.5 σ, from a 4.4 Å dataset (Table S3) collected from crystals of Csm1:Mam1$^{221\text{-}290}$ Y243M. Green density shows the locations of the sulfur atoms from Csm1 Met116 and Mam1 Met243, confirming the register and orientation of the Mam1 model.

(B) F_o-F_c simulated-annealing electron density map, contoured at 2.0 σ, calculated with Mam1 omitted.